



Enhancing CO₂-Valorization Using *Clostridium autoethanogenum* for Sustainable Fuel and Chemicals Production

James K. Heffernan^{1†}, Kaspar Valgepea^{1,2†}, Renato de Souza Pinto Lemgruber¹, Isabella Casini³, Manuel Plan⁴, Ryan Tappel⁵, Sean D. Simpson⁵, Michael Köpke⁵, Lars K. Nielsen^{1,4} and Esteban Marcellin^{1,4*}

¹ Australian Institute for Bioengineering and Nanotechnology, The University of Queensland, Saint Lucia, QLD, Australia, ² ERA Chair in Gas Fermentation Technologies, Institute of Technology, University of Tartu, Tartu, Estonia, ³ Center for Applied Geosciences, University of Tübingen, Tübingen, Germany, ⁴ Queensland Node of Metabolomics Australia, The University of Queensland, Saint Lucia, QLD, Australia, ⁵ LanzaTech Inc., Skokie, IL, United States

OPEN ACCESS

Edited by:

Christoph Herwig,
Vienna University of
Technology, Austria

Reviewed by:

Claudio Martin Pereira De Pereira,
Federal University of Pelotas, Brazil
Frank Robert Bengelsdorf,
University of Ulm, Germany

*Correspondence:

Esteban Marcellin
e.marcellin@uq.edu.au

[†]These authors have contributed
equally to this work

Specialty section:

This article was submitted to
Bioprocess Engineering,
a section of the journal
Frontiers in Bioengineering and
Biotechnology

Received: 18 July 2019

Accepted: 02 March 2020

Published: 27 March 2020

Citation:

Heffernan JK, Valgepea K, de Souza
Pinto Lemgruber R, Casini I, Plan M,
Tappel R, Simpson SD, Köpke M,
Nielsen LK and Marcellin E (2020)
Enhancing CO₂-Valorization Using
Clostridium autoethanogenum for
Sustainable Fuel and Chemicals
Production.
Front. Bioeng. Biotechnol. 8:204.
doi: 10.3389/fbioe.2020.00204

Acetogenic bacteria can convert waste gases into fuels and chemicals. Design of bioprocesses for waste carbon valorization requires quantification of steady-state carbon flows. Here, steady-state quantification of autotrophic chemostats containing *Clostridium autoethanogenum* grown on CO₂ and H₂ revealed that captured carbon (460 ± 80 mmol/gDCW/day) had a significant distribution to ethanol (54 ± 3 C-mol% with a 2.4 ± 0.3 g/L titer). We were impressed with this initial result, but also observed limitations to biomass concentration and growth rate. Metabolic modeling predicted culture performance and indicated significant metabolic adjustments when compared to fermentation with CO as the carbon source. Moreover, modeling highlighted flux to pyruvate, and subsequently reduced ferredoxin, as a target for improving CO₂ and H₂ fermentation. Supplementation with a small amount of CO enabled co-utilization with CO₂, and enhanced CO₂ fermentation performance significantly, while maintaining an industrially relevant product profile. Additionally, the highest specific flux through the Wood-Ljungdahl pathway was observed during co-utilization of CO₂ and CO. Furthermore, the addition of CO led to superior CO₂-valorizing characteristics (9.7 ± 0.4 g/L ethanol with a 66 ± 2 C-mol% distribution, and 540 ± 20 mmol CO₂/gDCW/day). Similar industrial processes are commercial or currently being scaled up, indicating CO-supplemented CO₂ and H₂ fermentation has high potential for sustainable fuel and chemical production. This work also provides a reference dataset to advance our understanding of CO₂ gas fermentation, which can contribute to mitigating climate change.

Keywords: gas fermentation, *Clostridium autoethanogenum*, carbon dioxide, valorization, carbon recycling, fuel and chemical platforms

INTRODUCTION

Gas fermentation has attractive waste carbon valorization properties, for which the need is intensifying (International Panel on Climate Change [IPCC], 2014; Emerson and Stephanopoulos, 2019). Recently, LanzaTech commercialized the first waste gas-to-ethanol process, efficiently incorporating the carbon from steel mill off-gas into fuel quality ethanol *via* the model acetogen

Clostridium autoethanogenum. The key carbon source—carbon monoxide (CO)—accounts for a significant portion of steel mill off-gas and synthesis gas (syngas), which can be generated from multiple high-volume, non-gaseous waste feedstocks (e.g., biomass, municipal solid waste) (Liew et al., 2016). Therefore, LanzaTech's process is significant in that it valorizes waste carbon by fusing two one-carbon gas molecules (C1) into liquid fuel. Furthermore, Handler et al. (2016) found that ethanol produced by LanzaTech's process reduced greenhouse gas emissions by 67 to 98% when compared to petroleum gasoline on an energy content and "cradle-to-grave" basis (feedstock dependent). Carbon dioxide (CO₂) represents a more diverse and plentiful waste stream compared to CO (International Panel on Climate Change [IPCC], 2014), thus embodying a feedstock with greater climate change mitigation and carbon recycling potential.

Increasing acetogenic carbon capture as CO₂ would build on the success of commercial gas fermentation and continue the expansion of the technology as a platform for sustainable chemical production (Redl et al., 2017; Bengelsdorf et al., 2018; Müller, 2019). Compared to other CO₂ valorization methods, acetogens are ideal candidates due to their high metabolic efficiency, ability to handle variable gas compositions, high product specificity, scalability, and low susceptibility to poisoning by sulfur, chlorine, and tars (Liew et al., 2016; Artz et al., 2018). However, metabolism of CO₂ requires an energy source, for which some see an appropriate solution is lacking (Emerson and Stephanopoulos, 2019).

Gas fermenting acetogens harbor the Wood-Ljungdahl pathway (WLP) (Drake et al., 2008), a non-photosynthetic C1-fixation metabolic pathway with the highest-known theoretical thermodynamic efficiency (Fast and Papoutsakis, 2012; Schuchmann and Müller, 2014; Müller, 2019). Various potential energy sources exist for metabolizing CO₂, primarily hydrogen, nitrates, sugars, and arginine. Yet, acetogenic CO₂ valorization, which is actively being developed for industrial implementation (Tizard and Sechrist, 2015), poses challenges along with promise. These include potential adenosine triphosphate (ATP) starvation in autotrophic conditions and carbon catabolite repression in hetero/mixotrophic conditions (Emerson and Stephanopoulos, 2019).

Hydrogen (H₂) is the most recognized energy source for CO₂ utilization—as metabolism of sugars or nitrates cause shifts in metabolism that result in lower CO₂ or H₂ utilization (Liew et al., 2016; Emerson and Stephanopoulos, 2019). H₂ production will also logically transition to renewable sources in the future, whereas production of sugars and nitrates are dependent on less-sustainable methods. Furthermore, leveled cost predictions for solar H₂ indicate a 30% reduction by 2030, potentially becoming competitive with the current leveled cost of fossil fuel derived H₂ by 2035 (Detz et al., 2018; Glenk and Reichelstein, 2019). This is in part due to rapidly decreasing solar electricity costs (IRENA, 2017) and projections of H₂ electrolysis technology development (Detz et al., 2018; Glenk and Reichelstein, 2019). Similarly, atmospheric CO₂ capture *via* direct air contact showed promising feasibility recently (Keith et al., 2018), which represents an essential development for carbon recycling (Otto et al., 2015). Various

power-to-gas technologies are being discussed for mediating fluctuations in renewable power generation (Götz et al., 2016). By extension, gas fermentation to liquid products could couple mediation of renewable power fluctuations to carbon recycling (Redl et al., 2017). This provides an attractive new opportunity for bacterial artificial-photosynthesis, whereby renewable H₂ supplementation facilitates acetogenic CO₂ valorization (Claassens et al., 2016; Haas et al., 2018).

Continuous culture bioprocesses are preferable to batch or fed-batch fermentation bioprocesses (Hoskisson and Hobbs, 2005). Furthermore, systems-level quantification is essential for design-build-test-learn bioprocess optimization by metabolic engineering (Valgepea et al., 2017). Therefore, obtaining quantitative datasets from steady-state chemostat cultures, whose analyses are comparable between experiments, is important for development of these systems (Adamberg et al., 2015). Whilst Bengelsdorf et al. (2018) reviewed autotrophic acetogen growth on CO₂ and H₂ (CO₂/H₂), and Mock et al. (2015) provided notable insight into the CO₂/H₂ metabolism of *C. autoethanogenum*, the literature lacks a steady-state dataset where carbon flows in a CO₂/H₂ fermentation are quantified. Here we aimed to quantify steady-state CO₂/H₂ fermentation using fully instrumented chemostats and the model acetogen *C. autoethanogenum*. Subsequently, we showed that CO₂ is a promising feedstock alternative to CO, as more than half of the substrate CO₂ carbon was converted into ethanol. Furthermore, supplementation with CO at low concentrations improved fermentation performance significantly.

MATERIALS AND METHODS

Bacterial Strain, Growth Medium, and Continuous Culture Conditions

A derivative of *Clostridium autoethanogenum* DSM 10061 strain—DSM 19630—deposited in the German Collection of Microorganisms and Cell Cultures (DSMZ) was used in all experiments and stored as glycerol stocks at -80°C . This non-commercial strain was grown on CO₂/H₂ ($\sim 23\%$ CO₂, $\sim 67\%$ H₂ and $\sim 10\%$ Ar; BOC Australia) and CO/CO₂/H₂ ($\sim 2\%$ CO, $\sim 23\%$ CO₂, $\sim 65\%$ H₂, and $\sim 10\%$ Ar; BOC Australia) in chemically defined medium (Valgepea et al., 2017). Cells were grown under strictly anaerobic conditions at 37°C and at a pH of 5 (maintained by 5 M NH₄OH). Chemostat continuous culture achieved steady-states at dilution rates (D) = 0.47 ± 0.01 (CO₂/H₂; specific growth rate (μ) = 0.0196 ± 0.0004 [average \pm standard deviation]), 0.5 ± 0.01 , and 1 ± 0.01 day⁻¹ (CO/CO₂/H₂; μ = 0.021 ± 0.0004 , and 0.042 ± 0.0008 h⁻¹ respectively). See **Table 1** for steady-state gas-liquid mass transfer rate data. The steady-state results reported here were collected after optical density (OD), gas uptake and production rates had been stable in chemostat mode for at least three working volumes. See Valgepea et al. (2017) for details on equipment.

Experimental Analysis and Quantification

Biomass concentration (gDCW/L) was estimated, and extracellular metabolome analysis carried out as specified in Valgepea et al. (2018).

TABLE 1 | Summary of low-biomass *Clostridium autoethanogenum* fermentations.

Gas	y	F	N	BR	D	BC	Ace		EtOH		
	(Ar to 100%)	mL/min	rpm	#	day ⁻¹	gDCW/L	±	g/L	±	g/L	±
CO ^a	60% CO	50	510	4	1	0.47	0.02	2.12	0.18	0.63	0.05
Syngas ^a	50 % CO, 20% CO ₂ , 20% H ₂	50	500	2	1	0.48	0.04	4.35	0.12	0.61	0.06
CO/H ₂ ^a	15% CO, 45% H ₂	50	650	4	1	0.46	0.04	0.69	0.07	4.46	0.41
CO/CO ₂ /H ₂	2% CO, 23% CO ₂ , 65% H ₂	30	1200	2	1	0.34	0.02	5.03	0.34	4.79	0.43
CO ₂ /H ₂	23% CO ₂ , 67% H ₂	32	500	3	0.5	0.18	0.02	2.51	0.42	2.36	0.25
CO/CO ₂ /H ₂	2% CO, 23% CO ₂ , 65% H ₂	30	800	2	0.5	0.54	0.01	5.97	0.98	9.69	0.39

^aData from Valgepea et al. (2018).

y, gas compositions; F, gas flowrate; N, stirrer speed; BR, biological replicates; D, dilution rate; BC, biomass concentration; Ace, acetate concentration; EtOH, ethanol concentration; ±, plus/minus standard deviation.

Bioreactor off-gas was analyzed by an online Hiden HPR-20-QIC mass spectrometer. The Faraday Cup detector monitored the intensities of H₂, CO, ethanol, H₂S, Ar, and CO₂ at 2, 14, 31, 34, 40, and 44 atomic mass units (amu), respectively, in the bioreactor off-gas. These masses were chosen so that each target compound would be represented by a unique signal. This was determined to be essential to achieve the highest confidence in quantification using preliminary experiments, as interferences from other compounds at a shared mass could not be reliably accounted for (e.g., the more intense signal from CO at 28 amu could not be used due to the uncertainty of interference at 28 amu from CO₂ fragmentation). Gas from the cylinder was used as the calibration gas for each MS-cycle (i.e., “online calibration”) to achieve reliable off-gas analysis (Valgepea et al., 2017).

Gas uptake (CO, CO₂, and H₂) and production (ethanol) were determined using “online calibration” of the MS by analyzing the respective feed gas directly from the cylinder after each analysis cycle of the bioreactors. Specific rates (mmol/gDCW/h) were calculated by taking into account the exact composition of the respective gas, bioreactor liquid working volume, feed gas flow rate, off-gas flow rate (based on the fractional difference of the inert gas [Ar] in the feed and off-gas composition), the ideal gas molar volume, and the steady-state biomass concentration.

The carbon balances were determined at 116 ± 11%, 103 ± 12%, and 108 ± 11% for CO₂/H₂, and CO/CO₂/H₂ at D = 0.5 and 1 day⁻¹ respectively (total C-mol products/total C-mol substrates), as specified in Valgepea et al. (2017).

Genome-Scale Metabolic Modeling With GEM iCLAU786

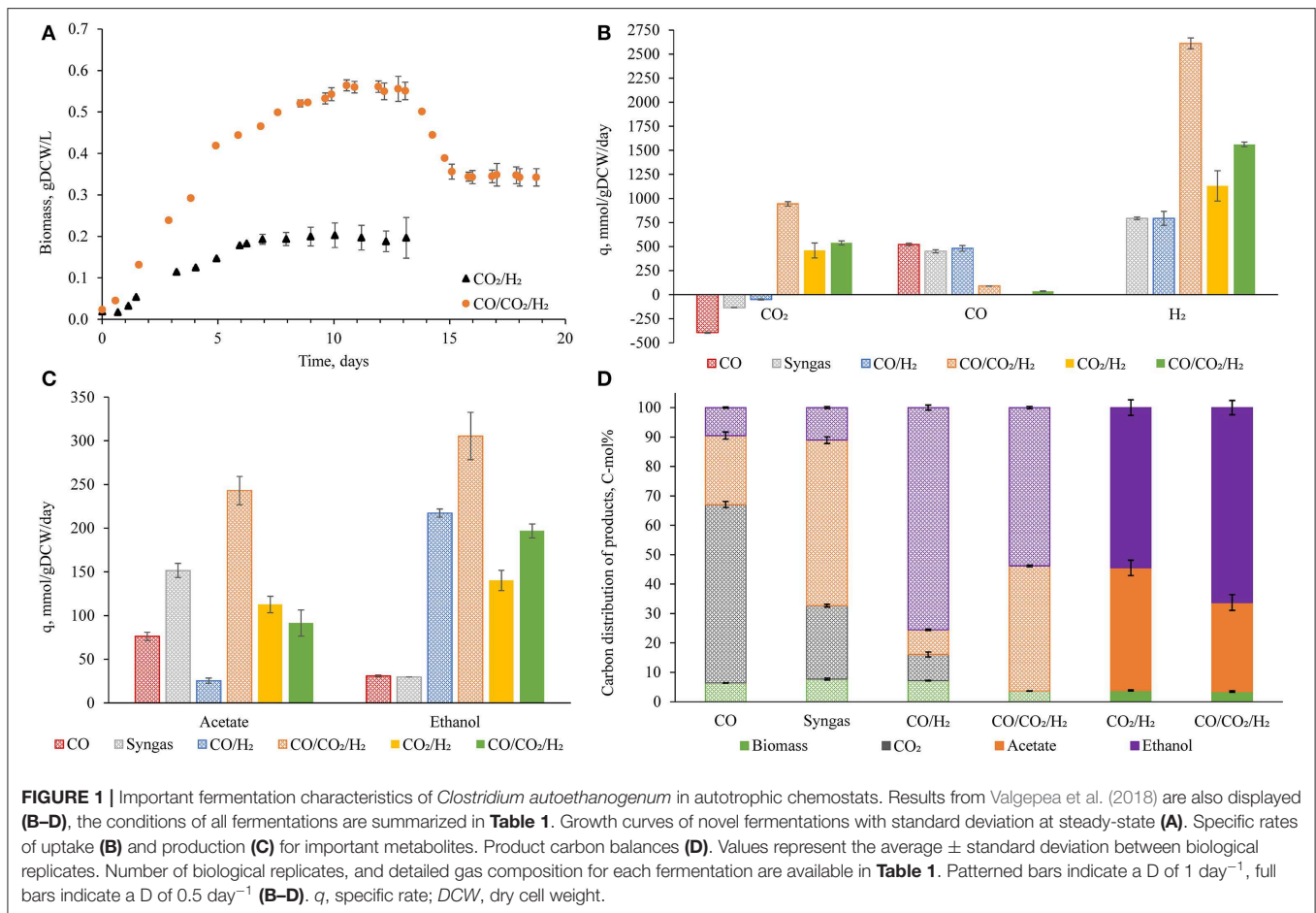
Model simulations were performed using genome scale model (GEM) iCLAU786 of *C. autoethanogenum* and flux balance analysis (FBA) (Orth and Palsson, 2011) as specified in Valgepea et al. (2018). Briefly, we used FBA to estimate intracellular fluxes (SIM1–26) by incorporating experimentally measured constraints (specific growth rate, and specific acetate, ethanol, cysteine, CO, CO₂, and H₂ consumption or production rates; **Table S3**) and employing maximization of ATP dissipation as the objective function. These values were validated by prediction of “optimal” growth phenotypes for

experimental conditions (SIM27–48), which incorporated experimental constraints (specific cysteine, CO, CO₂, and H₂ consumption rates), ATP dissipation flux calculated above, and maximization of biomass yield as the objective function. Complete simulation results identified as SIMx (e.g., SIM1) in the text are in **Table S11**. SIM1-19, 27-41, and 49-55 are from Valgepea et al. (2018). Additional constraints were also used to improve the accuracy of predictive simulations were justifiable [SIM49-55; details described in Valgepea et al. (2018)]. Here, CO₂ reduction to formate was forced from the formate dehydrogenase (FdhA) reaction scheme (Reaction ID: rxn00103_c0) in SIM42-48, to the correct reaction scheme in SIM56-62, as identified by Mock et al. (2015)—FdhA/Hydrogenase ABCDE complex (HytABCDE; Reaction ID: rxn08518_c0). Additionally, since extracellular metabolome analysis did not detect excretion of pyruvate by the cells, we manually blocked pyruvate export in the model (rxn05469_c0) in SIM56-62. Reaction IDs comprising letters and numbers are labels corresponding to reactions in **Table S11** (follows reference to reaction/enzyme).

RESULTS

Clostridium autoethanogenum Steady-State Fermentation of Carbon Dioxide and Hydrogen

Clostridium autoethanogenum cells reached steady-state when growing on CO₂/H₂ in chemostats at dilution rate (D) ~0.5 day⁻¹ [specific growth rate (μ) ~0.02 h⁻¹] with a biomass concentration of 0.18 ± 0.02 g dry cell weight (gDCW)/L (**Figure 1A**). It is important to note that attempts to reach a steady-state at D = 1 day⁻¹ were unsuccessful. Unlike the chemostat cultures of *C. autoethanogenum* with CO (Valgepea et al., 2017, 2018) and CO₂/H₂ retentostat cultures (Mock et al., 2015), the CO₂/H₂ cultures could not reach stable biomass concentrations before the culture began oscillation cycles; previously observed above ~1.6 gDCW/L (Valgepea et al., 2017). The physiological reason and mechanism for such oscillatory culture behavior are under investigation, but we assumed that cell recycling is a requirement for CO₂/H₂ culture stability. For example, Molitor et al. (2019) showed consistent, high-biomass



concentration and high-acetate CO₂/H₂ fermentation with *Clostridium ljungdahlii* in a retentostat with complete recycling.

Despite the attempt to reach a steady-state at D = 1 day⁻¹, cells reached steady-state at dilution rate = 0.5 day⁻¹, with a specific rate of carbon incorporation (i.e., q_{CO_2}) of 480 \pm 80 mmol/gDCW/day (Figure 1B). Furthermore, the specific production rates of ethanol and acetate were 140 \pm 10 and 113 \pm 9 mmol/gDCW/day, respectively (Figure 1C). Strikingly, this meant around half of the captured carbon was converted to ethanol (54 \pm 3 C mol%) (Figure 1D and Table S4). Fermentation conditions and titers are available in Table 1, showing an impressive ethanol concentration compared to previous fermentations where CO was the main carbon and energy source.

Despite the different dilution rate, the CO₂/H₂ results generated were compared to previously published chemostat cultures of *C. autoethanogenum* grown on CO, syngas, and CO/H₂ (Valgepea et al., 2018) at similar biomass concentrations (\sim 0.5 gDCW/L) (Figures 1B–D). Specific rates of acetate and ethanol production achieved here for CO₂/H₂ cultures fell between those for syngas (■) and CO/H₂ (■) cultures (Figures 1B,D). However, the specific rate of carbon incorporation was higher for CO₂/H₂ (Figure 1C). We found that more than half of the captured CO₂ was converted into

ethanol (Figure 1D). These results were encouraging, especially as ethanol production has unfavorable stoichiometry compared to acetate (Mock et al., 2015). Furthermore, the H₂ specific uptake rate (1,130 \pm 160 mmol/gDCW/day) showed that higher H₂ uptake rates are achievable (compared to old datasets). These results show that higher carbon yields are possible (Valgepea et al., 2018). To investigate further the metabolic demand and the feasibility of CO₂/H₂ fermentation, we utilized the measured specific consumption and production rates and specific growth rate from the steady-state dataset as constraints for the genome-scale metabolic model (GEM) to find candidate mechanisms for improving CO₂/H₂ fermentation using the metabolic model iCLAU786.

Metabolic Model of Carbon Dioxide and Hydrogen Fermentation

Estimation of intracellular processes constrained by *in vivo* datasets represents an important developmental step for progressing acetogenic CO₂ valorization. Here, we used the GEM to compare intracellular metabolic flux distributions on CO₂/H₂ and CO-containing gases (Figure 2). See Figures S2, S3 and Tables S8–S10 for further flux comparison summaries.

Intracellular metabolic fluxes estimated using the model iCLAU786 and flux balance analysis (FBA) (Figure 2) showed

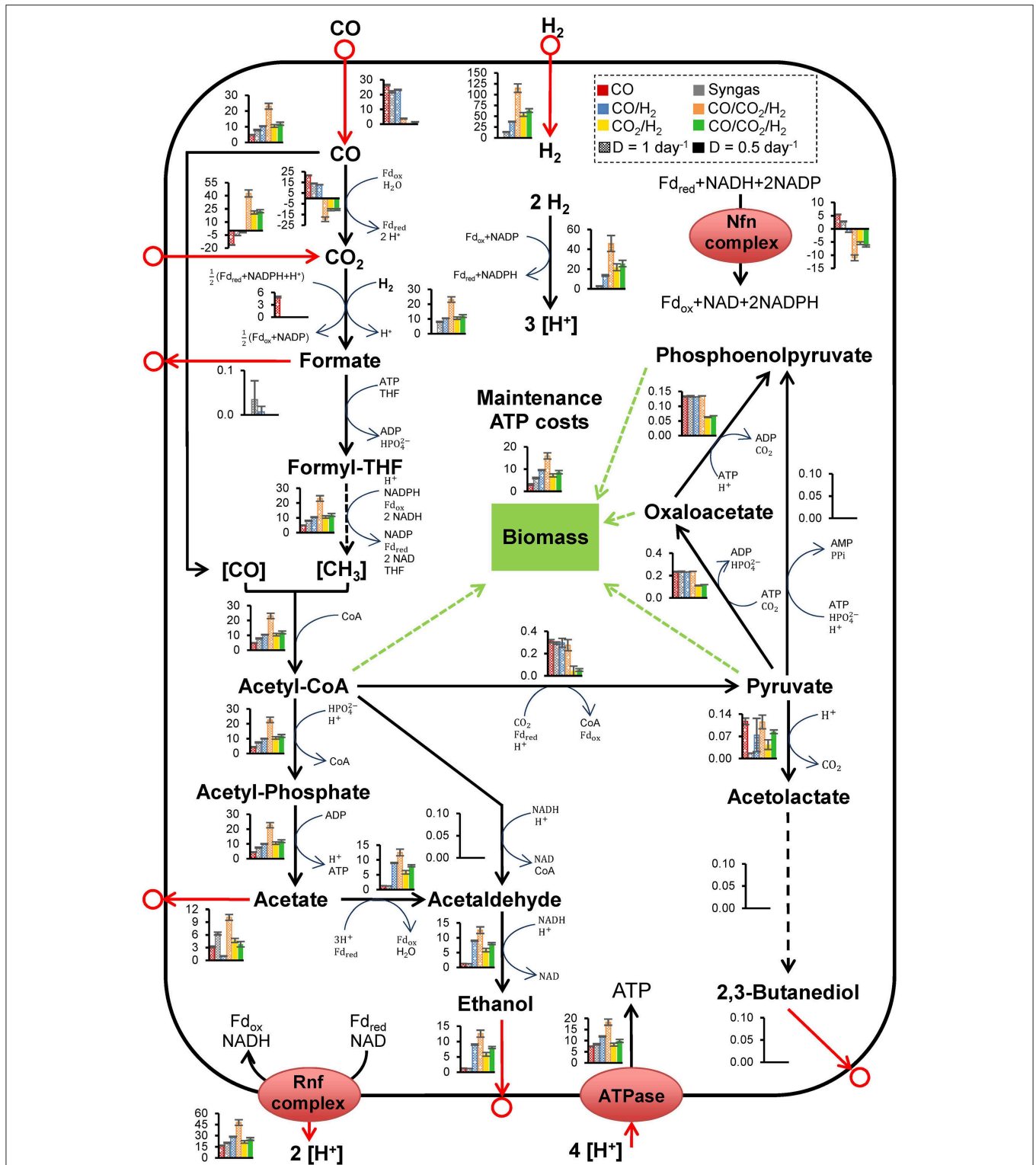


FIGURE 2 | Intracellular metabolic fluxes in *Clostridium autoethanogenum* growing on various gas mixes, estimated using the metabolic model iCLAU786 and flux balance analysis. Bar charts show specific flux rates (mmol/gDCW/h) from **Tables S10, S11** and represent the average \pm standard deviation between biological Replicates from SIM: 1–4 (CO), 9–10 (Syngas), 13–15 (CO/H₂), 20–21 (CO/CO₂/H₂), 22–24 (CO₂/H₂), and 25–26 (CO/CO₂/H₂). Results for CO, syngas, and CO/H₂ are low biomass condition data from Valgepea et al. (2018), the conditions of these fermentations are summarized in **Table 1**. Number of biological replicates, and detailed gas composition for each fermentation are available in **Table 1**. Arrows show the direction of calculated fluxes; red arrows denote uptake or secretion, dashed arrows denote a series of reactions. Brackets denote metabolites bound by an enzyme. Refer to **Figures S1, S2** for enzyme involvement, metabolite abbreviations, and complete flux balance analysis datasets.

remarkable similarity to the combined theoretical stoichiometry of acetate and ethanol production (Mock et al., 2015) and indicated energetic cofactor circuits with mapping close to 1:1 (experimental:theoretical stoichiometry; **Figure S4**). Ethanol production likely occurred *via* acetaldehyde:ferredoxin oxidoreductase (AOR; ReactionID: leq000004; see Materials and Methods) under autotrophic conditions, with the HytABCDE (leq000001) and Nfn complex (leq000002) likely facilitating cofactor production *via* electron bifurcation (**Figure 2**) (Valgepea et al., 2018). This is a mechanism for minimization of free energy loss employed by *C. autoethanogenum* and may play a key role in sustaining proton motive force by balancing acetate, ethanol, and ATP production (Mock et al., 2015; Valgepea et al., 2018). Engineering acetogens to redirect this energy toward cellular growth, sacrificing some ethanol production, could be beneficial for CO₂ fermentation (Emerson and Stephanopoulos, 2019).

It was notable that, unlike CO fermentations, the intracellular pyruvate:ferredoxin oxidoreductase (PFOR; rxn05938_c0; acetyl-CoA ↔ pyruvate) flux was not significantly in the direction of pyruvate (**Figure 2**) (Valgepea et al., 2018). Under autotrophic conditions, PFOR links the WLP to anabolic pathways associated with biomass (Furdui and Ragsdale, 2000), and therefore this indicated high cell-specific energetic limitation. From this observation, we hypothesized that CO supplementation could provide a potential solution, as CO oxidation would generate additional Fd_{red}. Furthermore, an ATP/H₂ flux ratio of ~0.15 was estimated using metabolic modeling here compared to an ATP/CO ratio of ~0.28 in CO only fermentations (Valgepea et al., 2018). Considering CO/H₂ and CO₂/H₂ fermentations had equal carbon-flux through the WLP (~10 mmol/gDCW/h; **Figure 2**), supplementation with renewable CO from CO₂ electrolysis could aid biomass formation and culture stability. A similar process (but CO fermentation) was detailed by Haas et al. (2018).

Clostridium autoethanogenum **Steady-State Fermentation of Carbon Dioxide and Hydrogen Supplemented With Carbon Monoxide**

To validate our modeling hypothesis, *Clostridium autoethanogenum* was cultured with a low concentration of carbon monoxide in addition to CO₂ and H₂ (CO/CO₂/H₂) in chemostats. A steady-state was reached at D = 0.5 day⁻¹ (μ ~0.02 h⁻¹), and at D = 1 day⁻¹ (μ ~0.04 h⁻¹; **Figure 1A**; biomass concentrations of 0.54 ± 0.01 and 0.34 ± 0.02 gDCW/L respectively). CO/CO₂/H₂ fermentations at a D = 1 day⁻¹ (CO/CO₂/H₂¹; superscript 1 denotes D of 1 day⁻¹) and at a D = 0.5 day⁻¹ (CO/CO₂/H₂^{0.5}; superscript 0.5 denotes D of 0.5 day⁻¹) showed simultaneous uptake of CO (89 ± 2 and 36 ± 4 mmol/gDCW/day, respectively) and CO₂ (940 ± 20 and 540 ± 20 mmol/gDCW/day, respectively) (**Figure 1B**). The co-utilization of both C1 gases is, to the best of our knowledge, an unquantified phenomenon. This led to a specific carbon incorporation (CO/CO₂/H₂¹—1030 ± 30 mmol/gDCW/day) larger than any other gas type (maximum of ~450 mmol/gDCW/day for fermentations with CO in Valgepea

et al. (2018) or CO₂/H₂ in this work). This also resulted in significant improvements to culture performance compared to CO₂/H₂ fermentations.

Compared to CO₂/H₂, CO/CO₂/H₂^{0.5} showed higher acetate and ethanol titers (**Table 1**) and specific productivities (**Figure 1C**), and a higher ethanol/acetate ratio (2.15 vs. 1.24 mol/mol respectively; **Tables S1, S2**). While at a similar biomass concentration (CO/CO₂/H₂¹ best comparison due to similarity in dilution rate), acetate and ethanol titers (**Table 1**), and specific productivities (**Figure 1C**) are greater than during fermentation of other CO-containing gases. When comparing to high biomass (~1.4 gDCW/L) CO cultures, CO-supplementation still performs impressively—CO/H₂ fermentation achieved a higher ethanol titer (11.6 ± 0.4 g/L), while CO and syngas fermentations were similar (3.9 ± 0.2 and 5.4 ± 0.3 g/L respectively; **Table S5**). Otherwise, all specific productivities were higher for CO/CO₂/H₂¹ (**Figure S3**). Furthermore, the distribution of carbon to ethanol was still >50% (53.8 ± 0.4% and 66 ± 2% for CO/CO₂/H₂¹ and CO/CO₂/H₂^{0.5}, respectively; **Figure 1D** and **Table S4**).

To understand the metabolic effects of supplementing CO, FBA was performed using the same conditions and alterations as for CO₂/H₂ (**Figure 2**). Notably, the WLP specific flux throughput for CO/CO₂/H₂¹ was ~2-fold greater than for any other gas type (including high-biomass Valgepea et al., 2018). Furthermore, for CO₂ fermentations, Nfn complex flux direction was opposite that of CO and syngas fermentations. CO/CO₂/H₂^{0.5} also showed significantly greater flux through the AOR, whilst specific WLP productivity was insignificantly different compared to CO₂/H₂.

DISCUSSION

Achieving steady-state continuous cultures using CO₂/H₂ mixtures, without cell recycling here, was challenging. Yet, compared to other organisms fermenting CO₂/H₂ with continuous medium exchange, *Clostridium autoethanogenum* performs well (**Table 2**). No direct comparisons can be made to other experiments due to variations in conditions, but *C. autoethanogenum* clearly achieves the highest ethanol production, with comparable quantities of carbonous products also. *Acetobacterium woodii*, along with *Sporomusa ovata*, were shown to perform well when compared to a wide range of acetogens under batch CO₂/H₂ conditions (Groher and Weuster-Botz, 2016). Yet, as evidenced by omission of *S. ovata* from **Table 2**, few continuous culture characterizations of acetogens are available—an essential step for validation of industrial robustness in gas fermentation. As discussed by Molitor et al. (2019), the lack of yeast extract or C_{≥2} substrates is also distinguishing between fermentations.

Notably, CO₂/H₂ cultures displayed higher variability between biological replicates compared to those of CO-containing gas mixtures (**Figure 1**) (Valgepea et al., 2017). This may indicate variable organism fitness, a trait previously discussed for *C. autoethanogenum* by Liew et al. (2016), who extensively covered numerous techniques used for enhancing gas fermentation including—coupling to other processes, adaptive

TABLE 2 | Summary of quantitative and continuous CO₂/H₂ fermentations.

Organism	Strain	Experimental conditions	Growth rate (day ⁻¹)	C _{Product} g[DCW]/L	Productivity g/L/day, (g/gDCW/day)	Ref.
<i>Acetobacterium woodii</i>	DSM 1030	1 L chemostat, D = 0.84 day⁻¹, 1,200 rpm, 30 L/h 17% CO₂, 40% H₂, 43% N₂, 1 atm, pH 7.0, 30°C, 4 g/L YE, n = 1	μ = 0.84	B = 1.1 A = 22.0	A = 19.1 (17.4)	1
		1 L batch retentostat, D = 1.68 day ⁻¹ , 1,200 rpm, 30 L/h 17% CO ₂ , 40% H ₂ , 43% N ₂ , 1 atm, pH 7.0, 30°C, 4 g/L YE, n = 1		B = 6.0 ^{a,b} A = 22.6	A = 40 (16.0 ^{a,b})	1
		†D = 4.2 day ⁻¹		B = 10.0 ^{a,b} A = 23.5	A = 95 (18.5 ^{a,b})	
		1 L batch retentostat, D = 8.4 day ⁻¹ , 1,200 rpm, 30 L/h 25% CO ₂ , 60% H ₂ , 15% N ₂ , 1 atm, pH 7.0, 30°C, 4 g/L YE, n = 1		B = 11.0 A = 17.6	A = 148 (20.3)	1 ^{b,c}
	pMTL84151 _act _{thiA}	0.85 L batch retentostat, D = 1 day ⁻¹ , 800 rpm, 30 L/h 20% CO ₂ and 80% H ₂ , pH 7.0, 30°C, 2 g/L YE, 10 g/L K-acetate, n = 1	μ = 0	B = 4.6 ^d A = 48.6 Ac = 3.0	Ac = 0.6 (0.1)	2
<i>Acetobacterium</i> sp.	BR446	Semi-batch retentostat, D = 24 day ⁻¹ , CO ₂ and H ₂ , medium not specified		B = 4.8 A = 3.0	A = 71.0 (14.7)	3
<i>Clostridium autoethanogenum</i>	DSM 19630	0.75 L chemostat, D = 0.5 day⁻¹, 500 rpm, 1.92 L/h 23% CO₂, 67% H₂, 10% Ar, 1 atm, pH 5, 37°C, DM, n = 3	μ = 0.5	B = 0.2 A = 2.5 E = 2.4	B = 0.1 A = 1.3 (6.8) E = 1.2 (6.4)	Here
		†800 rpm, 1.8 L/h 2% CO, 23% CO ₂ , 67% H ₂ , 10% Ar, n = 2	μ = 0.5	B = 0.5 A = 6.0 E = 9.7	B = 0.3 A = 3.0 (5.5) E = 6.3 (11.6)	
		†D = 1 day ⁻¹ , 1,200 rpm	μ = 1.0	B = 0.3 A = 5.0 E = 4.8	B = 0.3 A = 5.0 (14.6) E = 6.2 (18.1)	
		DSM 10061	1.3 L continuous retentostat, D = 4.9 day ⁻¹ , 21 L/h 23% CO ₂ , 65% H ₂ , 9.2% N ₂ , pH 5.3, 37°C, DM, 3.1 g/L ammonium acetate, n = 1	μ = 0.5	B = 1.8 A = 7.5 E = 6.3	A = 36.7 (20.0) E = 30.9 (16.9)
<i>Clostridium ljungdahlii</i>	DSM 13528	0.5 L chemostat, D = 0.29 day⁻¹, 300 rpm, 1.8 L/h 20% CO₂ and 80% H₂, pH 5.5, 37°C, DM, n = 3	μ = 0.29	B = 0.2^e A = 6.3 E = 1.8	A = 1.8 E = 0.5	5
		†DM with NaNO ₃ replacing NH ₄ Cl, n = 1	μ = 0.29	B = 0.3^{b,e} (pH 5.5) A = 13.4^b (pH 6.0) E = 5.0^b (pH 5.0)	A = 3.9 E = 1.4	
		1 L batch retentostat, D = 0.96 day ⁻¹ , 300 rpm, 7.2 L/h 20% CO ₂ and 80% H ₂ , pH 5.7, 35°C, DM, n = 1	μ = 0	B = 2.3 ^a A = 18.5	A = 17.7	6
<i>Moorella thermoacetica</i>	ATCC 49707	1 L BCR, D = 2.16 day ⁻¹ , 72 L/h 33% CO ₂ and 67% H ₂ , pH = 6.0, 60°C, 10 g/L YE, n = 1	μ = 0	B = 4.1 ^a A = 25.0 ^a	A = 54.0 (13.3) ^f	7
<i>Moorella</i> sp.	HUC22-1	0.5 L semi-continuous with cell retention, 500 rpm, continuous 20% CO ₂ and 80% H ₂ , 3.6 L/h, pH 6.2, 55°C, 1 g/L YE, n = 1	μ = 0	B = 1.5 A = 22.0 E = 0.3	A = 6.9 (10.4)	8

Ref. 1–8: (Kantzow et al., 2015; Hoffmeister et al., 2016; Morinaga and Kawada, 1990; Mock et al., 2015; Klask et al., 2019; Molitor et al., 2019; Hu et al., 2016; Sakai et al., 2005). C_{Product}, product concentration; D, dilution rate; YE, yeast extract; DM, defined medium; n, number of replicates; B, biomass; A, acetate; E, ethanol; Ac, acetone; BCR, bubble column reactor.

^aestimated from graph, ^bnot steady state (represented as maximum), ^ccell retention membrane was blocked before steady state was reached, ^dcalculated using data from Kantzow et al. (2015), ^ecalculated using data from Molitor et al. (2019), ^fcalculated using estimated data.

† Similar to experiment above, only differences in conditions are listed. Bolded experiments are chemostats. Only biomass concentrations use gDCW/L.

laboratory evolution, and metabolic engineering of acetogens using genetic tools. CO-supplementation could be a valuable option for enhancement as it overcomes inherent problems linked to engineering acetogens. Supplementation of low quantities of CO here stabilized the culture, enabled culturing at D = 1 day⁻¹, and achieved higher biomass concentration with a carbon incorporation larger than any other gas type—all without compromising by-product distribution.

While, Valgepea et al. (2018) found that syngas fermentation lead to CO-only fermentation at steady-state, we observed

co-utilization of CO and CO₂. Tizard and Sechrist (2015) have also shown co-utilization for *C. autoethanogenum* continuous cultures, and it seems that co-uptake may also occur for some points of syngas batch fermentation (Infantes et al., 2020). Co-utilization of sugars was found for *E. coli* in chemostats—where inhibition of consumption, but no change in induction time was observed (Standing et al., 1972). The WLP is most likely no different, in that metabolism of CO is preferential, yet the pathway can co-consume CO₂ under certain conditions.

Various efforts have been made toward enhancing CO₂(+H₂) fermentation to C_{≥2} products (**Table 2**) (Emerson and Stephanopoulos, 2019). Braun and Gottschalk (1981) first discovered the potential for enhancement when *Acetobacterium woodii* simultaneously consumed fructose and a headspace of CO₂/H₂ during batch cultivation. Growth and acetate production was high but no characterization of the headspace was performed. More recently, continuous glucose-supplemented CO₂/H₂ fermentation of *Moorella thermoacetica* by Park et al. (2019) did not lead to net uptake of CO₂. Furthermore, Jones et al. (2016) did not show net CO₂ uptake for a wide range of acetogens (not *A. woodii*) fermenting syngas and fructose. *A. woodii* generates a sodium ion (Na⁺) gradient (Hess et al., 2013) rather than a proton (H⁺) gradient for membranous ATP generation (Pierce et al., 2008; Poehlein et al., 2015; Bengelsdorf et al., 2018). This may highlight an important metabolic difference from other model acetogens—decoupling the resources of the WLP and membranous ATP generation pathways could facilitate fermentation of sugar and CO₂/H₂ simultaneously.

Other enhancements have also struggled to achieve net CO₂ uptake. Co-culture of *C. acetobutylicum* and *C. ljungdahlii* showed syntrophic metabolic coupling when fermenting glucose, fructose, and CO₂/H₂, but no net CO₂ uptake (Charubin and Papoutsakis, 2019). Addition of nitrate to batch CO₂/H₂ fermentation by *C. ljungdahlii*, increased biomass concentration and subsequently volumetric productivity of acetate (Emerson et al., 2019). However, the specific WLP productivity decreased, meaning lower utilization of CO₂. Other organisms not recognized as gas fermenters can also use mixotrophy to minimize carbon loss, such as *Clostridium beijerinckii* but have not displayed net CO₂ uptake either (Sandoval-Espinola et al., 2017). To the best of our knowledge, this is the first report where supplementation of a substrate other than H₂, increased productivities of continuous acetogenic CO₂ fermentation while maintaining net CO₂ utilization. Furthermore, the effect of CO supplementation on CO₂ utilization was superlinear, indicating a synergistic mechanism (Park et al., 2019). This is encouraging for development of bioprocesses valorizing CO₂.

Comparisons between fermentation datasets enables us to speculate about the positive effect of CO-supplementation on CO₂/H₂ fermentation. Although, addition of CO led to minimal metabolic shifts (**Figure 2**—CO₂/H₂ vs. CO/CO₂/H₂0.5 and **Figure S2**), FBA showed that CO supplementation caused significant increases to the reduced ferredoxin consumption by AOR and Rnf complex (leq000004 and M002, respectively) compared to CO₂/H₂ (**Figure 2**). The overflow model proposed by Richter et al. (2016) suggests that high NADH production via Rnf and Nfn complexes (leq000002) is also important for reducing AOR product inhibition. In this way, NADH facilitates fast metabolism of acetaldehyde to ethanol via alcohol dehydrogenase (Adh(E); rxn00543_c0). Decreasing the acetate concentration reduces acidification and the ATP cost for excreting acetate (Valgepea et al., 2018). Including acetaldehyde conversion to ethanol and association to acetic acid, this also leads to consumption of 2 H⁺ (4 here vs. 2 produced via CODH). Therefore, CO consumption decreases the intracellular H⁺ pool,

and following Le Chatelier's principle, drives HytABCDE activity. Indeed, the change in specific H₂ uptake relative to specific CO₂ uptake is greater than that of CO (for CO₂/H₂ vs. CO/CO₂/H₂0.5, **Table S7**). Subsequently, the relative gain in free energy from H₂ is ~4-fold greater than CO. We speculate this is ultimately responsible for the improved fitness of CO-supplemented CO₂/H₂ fermentation by *C. autoethanogenum*. We propose the following five critical factors to this enhanced metabolism: [1] metabolism of CO increases the intracellular pool of reduced ferredoxin; [2] this stimulates oxidation of ferredoxin, which if consumed by the AOR; [3] reduces ATP costs; and [4] decreases the H⁺ pool/acidification; which therefore [5] drives H₂ uptake for further reduction of ferredoxin. Evidently, additional understanding of acetogenic redox metabolism, from a thermodynamic perspective, is important for developing acetogenic CO₂-valorization as a platform industrial bioprocess (Cueto-Rojas et al., 2015).

Physicochemical properties could also play a key role in CO-supplementation enabling to achieve a stable CO₂/H₂ chemostat culture at D = 1 day⁻¹. Generation of a stable and large non-equilibrium is what drives microbial growth (Qian and Beard, 2005; Igamberdiev and Kleczkowski, 2009; Quémener and Bouchez, 2014) and gas-liquid mass transfer (Ma et al., 2005). For continuous culture of gas fermenting microbes, an inherent relationship between substrate mass transfer and culture growth exists (**Supplementary Materials Note 2.1**). An important parameter for these systems is the Gibbs free energy of a system (Cueto-Rojas et al., 2015). This describes the thermodynamic favorability of the reaction system—termed spontaneity. Here, analysis of experimental flux and Gibbs free energy suggests that CO₂/H₂ fermentation is infeasible ($\Delta\dot{G}_{OR^0} = 5.4 \text{ kJ/mol/day}$), whereas CO-supplemented CO₂/H₂ fermentation is feasible ($\Delta\dot{G}_{OR^0} = -12.3 \text{ kJ/mol/day}$; **Table S6**). Though these calculations use standard conditions, they do indicate how close CO₂/H₂ fermentation is to the thermodynamic limit of metabolism. Theoretically, minute and unobservable changes to chemostat CO₂/H₂ fermentation can disrupt the culture (Henry and Martin, 2016). Thus, increasing the free energy of central metabolism with CO-supplementation appears to keep metabolism in a spontaneous and stable state by increasing reduced ferredoxin production.

The mechanisms for achieving the 2-fold higher specific WLP flux throughput for CO/CO₂/H₂1 compared to others is less clear but appears to be linked to the difference in primary substrate. CO/CO₂/H₂1 and CO/H₂ are the most similar CO₂ and CO fermentations, respectively (D ~1 day⁻¹ and carbon to hydrogen feed ratio (~1:3); **Table 1**), and the maximum carbon incorporation per cell for CO/H₂ was roughly half of that of CO/CO₂/H₂1 (~450 vs. ~1,000 mmol/gDCW). Theoretically, cells will maximize carbon-to-redox metabolism by minimizing thermodynamic losses. CO supplementation to a CO₂/H₂ culture seems to facilitate this as (H₂/carbon)_{feed}-(H₂/carbon)_{flux} was ~0 mol/mol for CO/CO₂/H₂ fermentations only (**Table S2**)—an indication of the relative magnitude of carbon and redox metabolism. This suggests that high specific fluxes for CO/CO₂/H₂1 may be a result of (close to) optimal co-factor recycling by *C. autoethanogenum*'s WLP and redox pathway.

Thus, the lower energy associated with CO₂ fermentation may, counterintuitively, stimulate specific WLP activity when in the presence of appropriate energy-containing substrates. Further quantifications of CO₂ metabolism and characterizations of enzyme activities are required to confirm these hypotheses (**Supplementary Materials Note 2.2**), as they assist our ability to engineer the links between redox and carbon metabolisms.

We established a dataset quantifying steady-state of the model acetogen *C. autoethanogenum* during autotrophic-CO₂/H₂ growth in chemostat cultures. This enabled analysis *via* FBA, and highlighted CO as a potential supplement. CO supplementation successfully improved metabolic stability and CO₂ utilization. This was the first time that intracellular fluxes for net uptake of CO₂ (with enhancement) were characterized. Industry is actively developing gas fermentation to valorize CO₂ (Tizard and Sechrist, 2015; Haas et al., 2018). Previously, genetic and process engineering of gas fermentation successfully developed the technology for industrial CO valorization (Liew et al., 2016). Therefore, progression to industrial CO₂ valorization is foreseeable, and CO supplementation may play a role in the continuing diversification of industrial gas fermentation.

DATA AVAILABILITY STATEMENT

All datasets generated for this study are included in the article/**Supplementary Material**.

AUTHOR CONTRIBUTIONS

All authors viewed and approved the manuscript and contributed significantly to the work. KV, EM, and LN conceived the project. JH, KV, and EM designed the experiments and analyzed the results. JH and KV performed experiments, supported by RS, IC,

MP, and EM. JH wrote the manuscript with the help of KV, EM, RT, SS, MK, and LN.

FUNDING

This study was funded by a Grant from the Australian Research Council, partly funded by LanzaTech (ARC LP140100213).

ACKNOWLEDGMENTS

Elements of this research utilized equipment and support provided by the Queensland node of Metabolomics Australia, an initiative of the Australian Government being conducted as part of the NCRIS National Research Infrastructure for Australia. IC would like to acknowledge support from the German Academic Exchange Service (DAAD) through the DAAD Kurzzstipendien für Doktoranden. We thank the following investors in LanzaTech's technology: Sir Stephen Tindall, Khosla Ventures, Qiming Venture Partners, Softbank China, the Malaysian Life Sciences Capital Fund, Mitsui, Primetals, CICC Growth Capital Fund I, L.P. and the New Zealand Superannuation Fund. There was no funding support from the European Union for the experimental part of the study. However, KV acknowledges support also from the European Union's Horizon 2020 research and innovation programme under grant agreement N810755.

SUPPLEMENTARY MATERIAL

The Supplementary Material for this article can be found online at: <https://www.frontiersin.org/articles/10.3389/fbioe.2020.00204/full#supplementary-material>

REFERENCES

- Adamberg, K., Valgepea, K., and Vilu, R. (2015). Advanced continuous cultivation methods for systems microbiology. *Microbiology* 161, 1707–1719. doi: 10.1099/mic.0.000146
- Artz, J., Müller, T. E., Thenert, K., Kleinekorte, J., Meys, R., Sternberg, A., et al. (2018). Sustainable conversion of carbon dioxide: an integrated review of catalysis and life cycle assessment. *Chem. Rev.* 118, 434–504. doi: 10.1021/acs.chemrev.7b00435
- Bengelsdorf, F. R., Beck, M. H., Erz, C., Hoffmeister, S., Karl, M. M., Riegler, P., et al. (2018). Bacterial anaerobic synthesis gas (syngas) and CO₂ + H₂ fermentation. *Adv. Appl. Microbiol.* 103, 143–221. doi: 10.1016/bs.aambs.2018.01.002
- Braun, K., and Gottschalk, G. (1981). Effect of molecular hydrogen and carbon dioxide on chemo-organotrophic growth of *Acetobacterium woodii* and *Clostridium aceticum*. *Arch. Microbiol.* 128, 294–298. doi: 10.1007/BF00422533
- Charubin, K., and Papoutsakis, E. T. (2019). Direct cell-to-cell exchange of matter in a synthetic *Clostridium* syntrophy enables CO₂ fixation, superior metabolite yields, and an expanded metabolic space. *Metab. Eng.* 52, 9–19. doi: 10.1016/j.ymben.2018.10.006
- Claessens, N. J., Sousa, D. Z., dos Santos, V. A. P. M., de Vos, W. M., and van der Oost, J. (2016). Harnessing the power of microbial autotrophy. *Nat. Rev. Microbiol.* 14, 692–706. doi: 10.1038/nrmicro.2016.130
- Cueto-Rojas, H. F., van Maris, A. J., Wahl, S. A., and Heijnen, J. J. (2015). Thermodynamics-based design of microbial cell factories for anaerobic product formation. *Trends Biotechnol.* 33, 534–546. doi: 10.1016/j.tibtech.2015.06.010
- Detz, R. J., Reek, J. N. H., and Van Der Zwaan, B. C. C. (2018). The future of solar fuels: when could they become competitive? *Energy Environ. Sci.* 11, 1653–1669. doi: 10.1039/C8EE00111A
- Drake, H. L., Gößner, A. S., and Daniel, S. L. (2008). Old acetogens, new light. *Ann. N. Y. Acad. Sci.* 1125, 100–128. doi: 10.1196/annals.1419.016
- Emerson, D. F., and Stephanopoulos, G. (2019). Limitations in converting waste gases to fuels and chemicals. *Curr. Opin. Biotechnol.* 59, 39–45. doi: 10.1016/j.copbio.2019.02.004
- Emerson, D. F., Woolston, B. M., Liu, N., Donnelly, M., Currie, D. H., and Stephanopoulos, G. (2019). Enhancing hydrogen-dependent growth of and carbon dioxide fixation by *Clostridium ljungdahli* through nitrate supplementation. *Biotechnol. Bioeng.* 116, 294–306. doi: 10.1002/bit.26847
- Fast, A. G., and Papoutsakis, E. T. (2012). Stoichiometric and energetic analyses of non-photosynthetic CO₂-fixation pathways to support synthetic biology strategies for production of fuels and chemicals. *Curr. Opin. Chem. Eng.* 1, 380–395. doi: 10.1016/j.coche.2012.07.005
- Furdui, C., and Ragsdale, S. W. (2000). The role of pyruvate ferredoxin oxidoreductase in pyruvate synthesis during autotrophic growth by the Wood-Ljungdahl pathway. *J. Biol. Chem.* 275, 28494–28499. doi: 10.1074/jbc.M003291200
- Glenk, G., and Reichelstein, S. (2019). Economics of converting renewable power to hydrogen. *Nat. Energy* 4, 216–222. doi: 10.1038/s41560-019-0326-1
- Götz, M., Lefebvre, J., Mörs, F., McDaniel Koch, A., Graf, F., Bajohr, S., et al. (2016). Renewable power-to-gas: a technological and economic review. *Renew. Energy* 85, 1371–1390. doi: 10.1016/j.renene.2015.07.066

- Groher, A., and Weuster-Botz, D. (2016). Comparative reaction engineering analysis of different acetogenic bacteria for gas fermentation. *J. Biotechnol.* 228, 82–94. doi: 10.1016/j.jbiotec.2016.04.032
- Haas, T., Krause, R., Weber, R., Demler, M., and Schmid, G. (2018). Technical photosynthesis involving CO₂ electrolysis and fermentation. *Nat. Catal.* 1, 32–39. doi: 10.1038/s41929-017-0005-1
- Handler, R. M., Shonnard, D. R., Griffing, E. M., Lai, A., and Palou-Rivera, I. (2016). Life cycle assessments of ethanol production via gas fermentation: anticipated greenhouse gas emissions for cellulosic and waste gas feedstocks. *Ind. Eng. Chem. Res.* 55, 3253–3261. doi: 10.1021/acs.iecr.5b03215
- Henry, A., and Martin, O. C. (2016). Short relaxation times but long transient times in both simple and complex reaction networks. *J. R. Soc. Interface* 13:20160388. doi: 10.1098/rsif.2016.0388
- Hess, V., Schuchmann, K., and Müller, V. (2013). The ferredoxin: NAD⁺ oxidoreductase (Rnf) from the acetogen *Acetobacterium woodii* requires na⁺ and is reversibly coupled to the membrane potential. *J. Biol. Chem.* 288, 31496–31502. doi: 10.1074/jbc.M113.510255
- Hoffmeister, S., Gerdomb, M., Bengelsdorf, F. R., Linder, S., Flüchter, S., Öztürk, H., et al. (2016). Acetone production with metabolically engineered strains of *Acetobacterium woodii*. *Metab. Eng.* 36, 37–47. doi: 10.1016/j.ymben.2016.03.001
- Hoskisson, P. A., and Hobbs, G. (2005). Continuous culture - making a comeback? *Microbiology* 151, 3153–3159. doi: 10.1099/mic.0.27924-0
- Hu, P., Chakraborty, S., Kumar, A., Woolston, B. M., Liu, H., Emerson, D., et al. (2016). Integrated bioprocess for conversion of gaseous substrates to liquids. *Proc. Natl. Acad. Sci. U.S.A.* 113, 2–7. doi: 10.1073/pnas.1516867113
- Igamberdiev, A. U., and Kleczkowski, L. A. (2009). Metabolic systems maintain stable non-equilibrium via thermodynamic buffering. *Bioessays* 31, 1091–1099. doi: 10.1002/bies.200900057
- Infantes, A., Kugel, M., and Neumann, A. (2020). Effect of cysteine, yeast extract, pH regulation and gas flow on acetate and ethanol formation and growth profiles of *Clostridium ljungdahlii* syngas fermentation. *BioRxiv[Preprint]*. doi: 10.1101/2020.01.13.904292
- International Panel on Climate Change [IPCC] (2014). *Climate Change 2014: Mitigation of Climate Change*.
- IRENA (2017). *Renewable Power Generation Costs in 2017*. Abu Dhabi: International Renewable Energy Agency.
- Jones, S. W., Fast, A. G., Carlson, E. D., Wiedel, C. A., Au, J., Antoniewicz, M. R., et al. (2016). CO₂ fixation by anaerobic non-photosynthetic mixotrophy for improved carbon conversion. *Nat. Commun.* 7:12800. doi: 10.1038/ncomms12800
- Kantow, C., Mayer, A., and Weuster-Botz, D. (2015). Continuous gas fermentation by *Acetobacterium woodii* in a submerged membrane reactor with full cell retention. *J. Biotechnol.* 212, 11–18. doi: 10.1016/j.jbiotec.2015.07.020
- Keith, D. W., Holmes, G., Angelo, D. St., and Heidel, K. (2018). A process for capturing CO₂ from the atmosphere. *Joule* 2, 1573–1594. doi: 10.1016/j.joule.2018.05.006
- Klask, C., Kliem-kuster, N., Molitor, B., and Angenent, L. T. (2019). An open-source multiple-bioreactor system for replicable gas-fermentation experiments: nitrate feed results in stochastic inhibition events, but improves ethanol production of *Clostridium ljungdahlii* with CO₂ and H₂. *BioRxiv[Preprint]*. doi: 10.1101/2019.12.15.877050
- Liew, F. M., Martin, E., Tappel, R., Heijstra, B., Mihalcea, C., and Köpke, M. (2016). Gas fermentation – a flexible platform for commercial scale production of low carbon fuels and chemicals from waste and renewable feedstocks. *Front. Microbiol.* 7:694. doi: 10.3389/fmicb.2016.00694
- Ma, Y., Yu, G., and Li, H. Z. (2005). Note on the mechanism of interfacial mass transfer of absorption processes. *Int. J. Heat Mass Transf.* 48, 3454–3460. doi: 10.1016/j.ijheatmasstransfer.2005.03.008
- Mock, J., Zheng, Y., Mueller, A. P., Ly, S., Tran, L., Segovia, S., et al. (2015). Energy conservation associated with ethanol formation from H₂ and CO₂ in *Clostridium autoethanogenum* involving electron bifurcation. *J. Bacteriol.* 197, 2965–2980. doi: 10.1128/JB.00399-15
- Molitor, B., Mishra, A., and Angenent, L. T. (2019). Power-to-protein: converting renewable electric power and carbon dioxide into single cell protein with a two-stage bioprocess. *Energy Environ. Sci.* 12, 3515–3521. doi: 10.1039/C9EE02381J
- Morinaga, T., and Kawada, N. (1990). The production of acetic acid from carbon dioxide and hydrogen by an anaerobic bacterium. *J. Biotechnol.* 14, 187–194. doi: 10.1016/0168-1656(90)90007-X
- Müller, V. (2019). New horizons in acetogenic conversion of one-carbon substrates and biological hydrogen storage. *Trends Biotechnol.* 37, 1344–1354. doi: 10.1016/j.tibtech.2019.05.008
- Orth, J. D., and Palsson, B. Ø. (2011). What is flux balance analysis? *Nat. Biotechnol.* 28, 245–248. doi: 10.1038/nbt.1614
- Otto, A., Grube, T., Schiebahn, S., and Stolten, D. (2015). Closing the loop: captured CO₂ as a feedstock in the chemical industry. *Energy Environ. Sci.* 8, 3283–3297. doi: 10.1039/C5EE02591E
- Park, J. O., Liu, N., Holinski, K. M., Emerson, D. F., Qiao, K., Woolston, B. M., et al. (2019). Synergistic substrate cofeeding stimulates reductive metabolism. *Nat. Metab.* 1, 643–651. doi: 10.1038/s42255-019-0077-0
- Pierce, E., Xie, G., Barabote, R. D., Saunders, E., Han, C. S., Detter, J. C., et al. (2008). The complete genome sequence of *Moorella thermoacetica* (f. *Clostridium thermoaceticum*). *Environ. Microbiol.* 10, 2550–2573. doi: 10.1111/j.1462-2920.2008.01679.x
- Poehlein, A., Cebulla, M., Ilg, M. M., Bengelsdorf, F. R., Schiel-bengelsdorf, B., Whited, G., et al. (2015). The complete genome sequence of *Clostridium acetatum*: a missing link between Rnf- and cytochrome-containing autotrophic acetogens. *MBio* 6:e01168-15. doi: 10.1128/mBio.01168-15
- Qian, H., and Beard, D. A. (2005). Thermodynamics of stoichiometric biochemical networks in living systems far from equilibrium. *Biophys. Chem.* 114, 213–220. doi: 10.1016/j.bpc.2004.12.001
- Quémener, E. D. Le., and Bouchez, T. (2014). A thermodynamic theory of microbial growth. *ISME J.* 8, 1747–1751. doi: 10.1038/ismej.2014.7
- Redl, S., Diender, M., Jensen, T. Ø., Sousa, D. Z., and Nielsen, A. T. (2017). Exploiting the potential of gas fermentation. *Ind. Crops Prod.* 106, 21–30. doi: 10.1016/j.indcrop.2016.11.015
- Richter, H., Molitor, B., Wei, H., Chen, W., Aristilde, L., and Angenent, L. T. (2016). Ethanol production in syngas-fermenting *Clostridium ljungdahlii* is controlled by thermodynamics rather than by enzyme expression. *Energy Environ. Sci.* 9, 2392–2399. doi: 10.1039/C6EE01108J
- Sakai, S., Nakashimada, Y., Inokuma, K., Kita, M., Okada, H., and Nishio, N. (2005). Acetate and ethanol production from H₂ and CO₂ by *Moorella* sp. using a repeated batch culture. *J. Biosci. Bioeng.* 99, 252–258. doi: 10.1263/jbb.99.252
- Sandoval-Espinola, W. J., Chinn, M. S., Thon, M. R., and Bruno-Bárcena, J. M. (2017). Evidence of mixotrophic carbon-capture by n-butanol-producer *Clostridium beijerinckii*. *Sci. Rep.* 7, 1–13. doi: 10.1038/s41598-017-12962-8
- Schuchmann, K., and Müller, V. (2014). Autotrophy at the thermodynamic limit of life: a model for energy conservation in acetogenic bacteria. *Nat. Rev. Microbiol.* 12, 809–821. doi: 10.1038/nrmicro3365
- Standing, C. N., Fredrickson, A. G., and Tsuchiya, H. M. (1972). Batch- and continuous-culture transients for two substrate systems. *Appl. Microbiol.* 23, 354–359. doi: 10.1128/AEM.23.2.354-359.1972
- Tizard, J. H., and Sechrist, P. A. (2015). *Carbon Capture in Fermentation*. U.S. Patent No 0,111,266. Washington, DC: U.S. Patent and Trademark Office. Available online at: <https://patents.justia.com/patent/20150111266>
- Valgepea, K., De Souza Pinto Lemgruber, R., Abdalla, T., Binos, S., Takemori, N., Takemori, A., et al. (2018). H₂ drives metabolic rearrangements in gas-fermenting *Clostridium autoethanogenum*. *Biotechnol. Biofuels* 11:55. doi: 10.1186/s13068-018-1052-9
- Valgepea, K., de Souza Pinto Lemgruber, R., Meaghan, K., Palfreyman, R. W., Abdalla, T., Heijstra, B. D., et al. (2017). Maintenance of ATP homeostasis triggers metabolic shifts in gas-fermenting acetogens. *Cell Syst.* 4, 505–515.e5. doi: 10.1016/j.cels.2017.04.008

Conflict of Interest: LanzaTech has interest in commercializing gas fermentation with *C. autoethanogenum*. RT, SS, and MK are employees of LanzaTech.

Copyright © 2020 Heffernan, Valgepea, de Souza Pinto Lemgruber, Casini, Plan, Tappel, Simpson, Köpke, Nielsen and Marcellin. This is an open-access article distributed under the terms of the Creative Commons Attribution License (CC BY). The use, distribution or reproduction in other forums is permitted, provided the original author(s) and the copyright owner(s) are credited and that the original publication in this journal is cited, in accordance with accepted academic practice. No use, distribution or reproduction is permitted which does not comply with these terms.